

Supplementary Data:

Effect of Electrostatics on Aggregation of Prion Protein Sup35 Peptide

Alexander M. Portillo¹, Alexey V. Krasnoslobodtsev¹, Yuri L. Lyubchenko^{1}*

¹ Department of Pharmaceutical Sciences, College of Pharmacy, COP 1012, University of Nebraska Medical Center, 986025 Nebraska Medical Center, Omaha, NE 68198-6025

*Corresponding Author: lyubchenko@unmc.edu

Contents:

s1. Single-molecule force spectroscopy data analysis. Comparison of Freely-Joined Chain and Worm Like Chain models.

s2. Comparison of parameters obtained from fitting of experimental force-distance curves.

s3. Kinetic curve of the prion peptide aggregation in water resulting from ThT fluorescence.

s4. Kinetic curves of the peptide aggregation at different pHs.

s5. AFM images of the aggregates formed in low salt buffers.

s6. AFM images (indicated with “i”) of the aggregates formed in high salt buffers.

Table s1. Parameters of dynamic force spectra for proline mutant (PepP).

s1. Single-molecule force spectroscopy data analysis. Comparison of Freely-Joined Chain and Worm Like Chain models.

The interactions between peptides were measured using single molecule force spectroscopy. AFM tip functionalized with peptide through PEG linker probes mica surface functionalized with the same peptide at various spots. Peptides interact with each other under conditions favorable upon approach cycle. These specific interactions are ruptured upon withdrawal of the tip from the surface. The rupture event produces a specific signature in the force-distance curve indicated with an arrow on Fig. s1. The part of the force-distance curve preceding the rupture point is associated with stretching of the flexible PEG linkers under applied force. Both worm like chain (WLC) and freely joined chain (FJC) were used to approximate the stretching of the linkers. Both models fitted data well, and when used for analysis of dynamic force spectroscopy, both also showed a similar trend. Figure s2 shows comparison of parameters obtained from the fit of experimental force-distance curves with WLC (first row) and FJC (second row). The distribution of measured values are similar for both models $L_c(\text{WLC})=34\text{nm}$ and $L_c(\text{FJC})=29\text{nm}$, persistence length is 0.17 nm, obtained from WLC fit and it is twice smaller than Kuhn length, 0.34 nm, determined from FJC fit. It was noted, however, that when both FJC and WLC models were used to fit experimental force-distance curves, WLC model provided consistently better fits based on residual RMS (root mean square) values in a wide range of pulling velocities in contrast to FJC. Additionally, WLC fits better the slope of the force-distance curve at the rupture point (frame 3) providing more accurate determination of the loading rate.

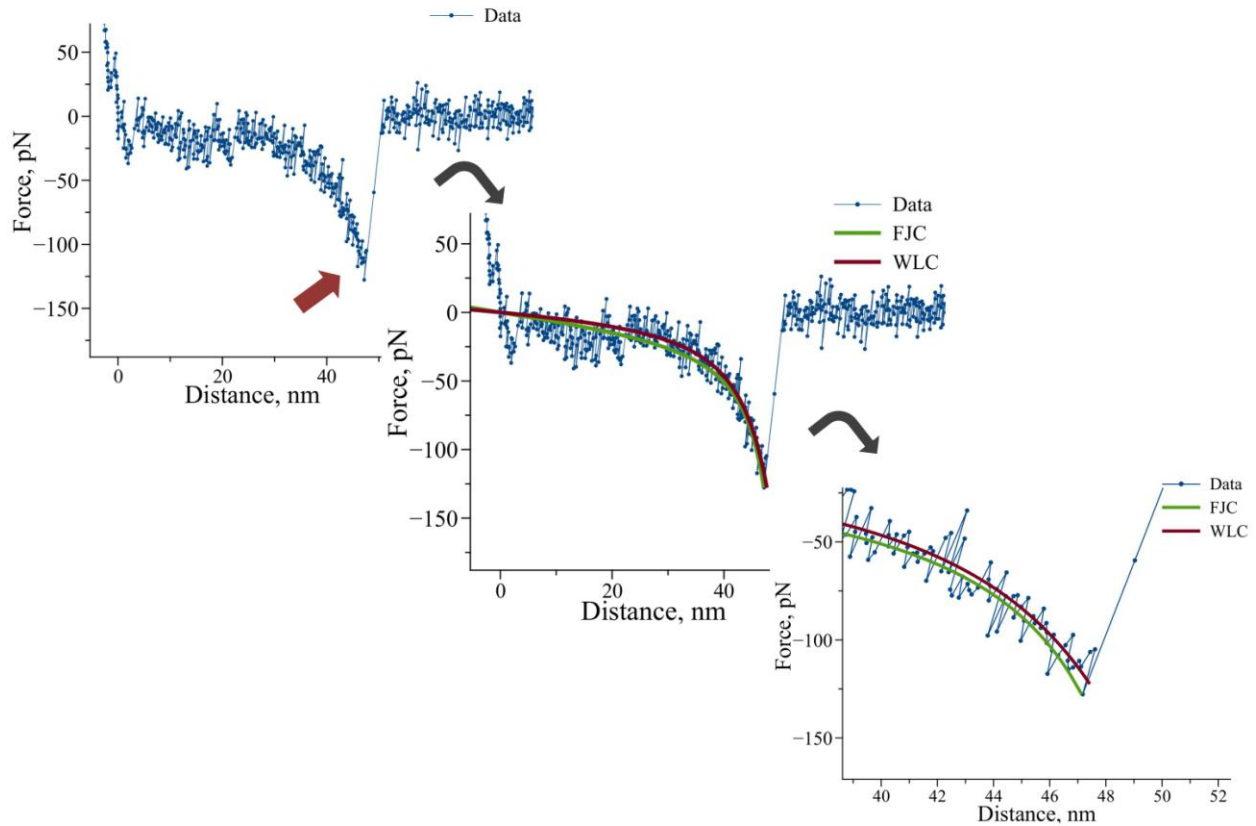


Figure s1. The rupture event indicated by an arrow in frame 1 shows a typical response of stretchable PEG linkers under applied external force. This part of the curve is then fitted with a model describing mechanical properties of the polymer (frame 2). Worm Like Chain (red) or Freely Joined Chain (green) were used to fit parts of the force-distance curves preceding the rupture point. Such analysis provides the following characteristics of the polymer chain: contour length of the polymer as well as persistence length (in WLC) or Kuhn length (in FJC). Frame 3 shows that WLC fits the curve better than FJC model, especially at the rupture point where apparent loading rate is estimated. Residual RMSs for the presented curve are 9.5 pN and 10.1 pN for WLC and FJC models, respectively.

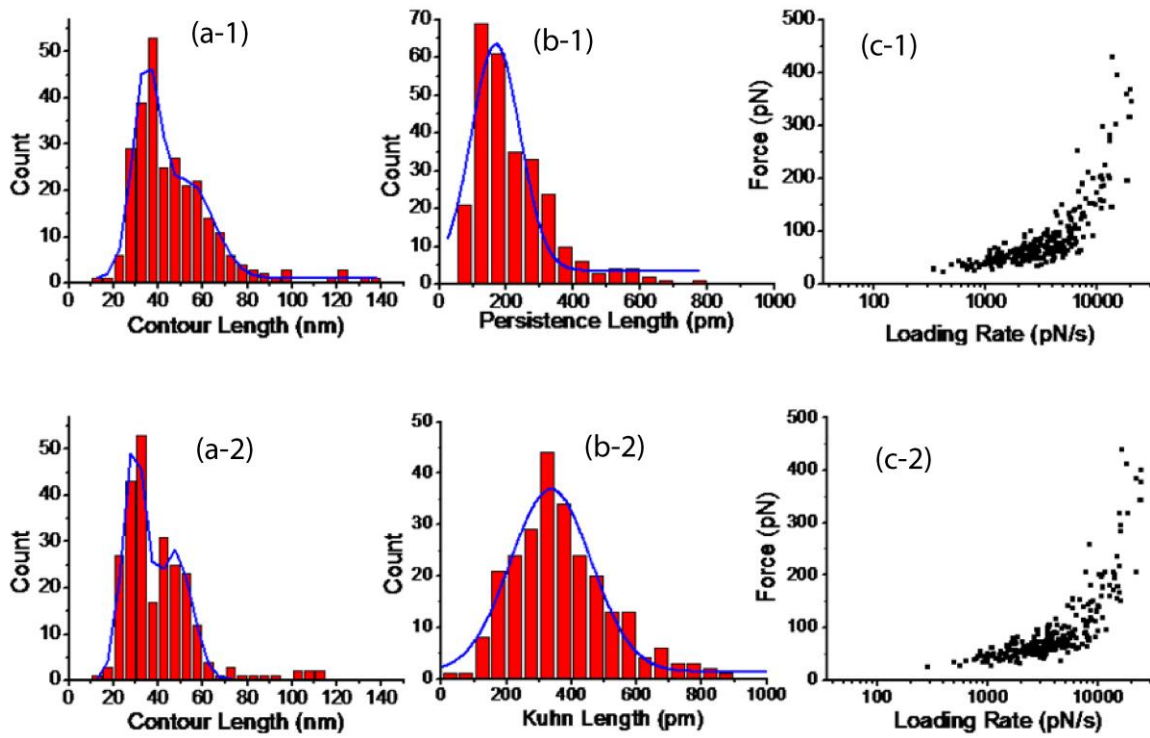


Figure s2. Comparison of parameters obtained from fitting of experimental force-distance curves. Worm Like Chain: a-1) Contour length, b-1) Persistence length, c-1) Dynamic force spectrum. Freely Joined Chain: a-2) Contour length, b-2) Kuhn length, c-2) Dynamic force spectrum.

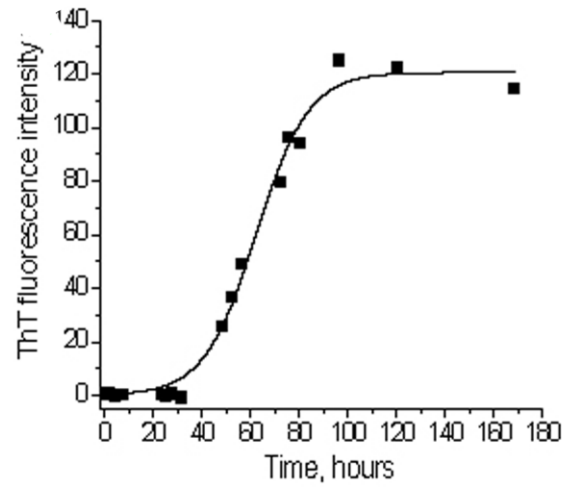


Figure s3. Kinetic curve of the prion peptide aggregation in water resulting from ThT fluorescence.

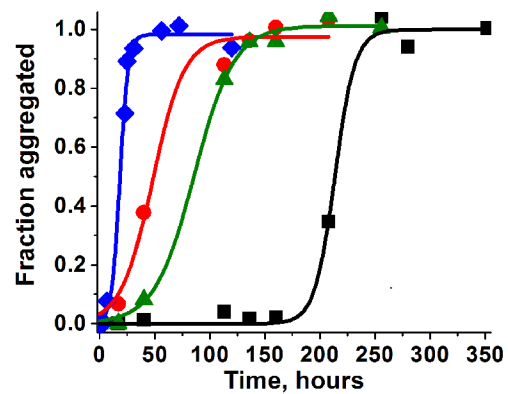


Figure s4. Kinetic curves of the peptide aggregation at different pHs shown in black squares (pH2.0), red circles (pH 3.7), blue diamonds (pH 5.6), and green triangles (pH 7.0).

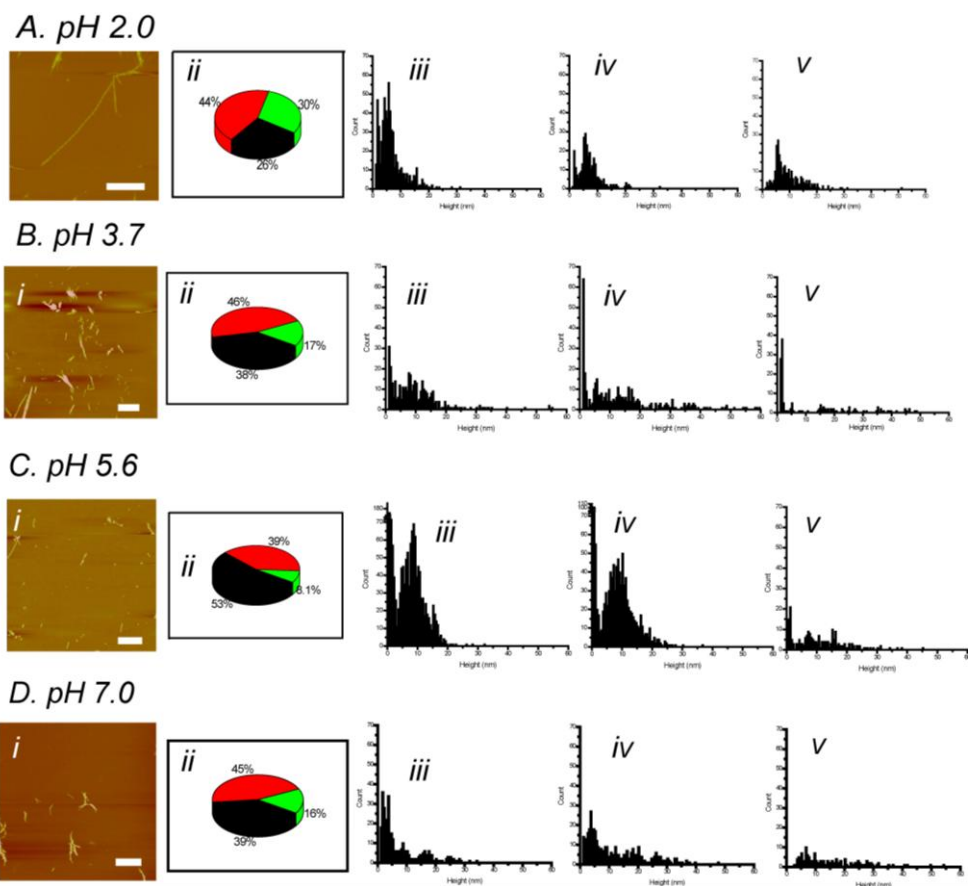
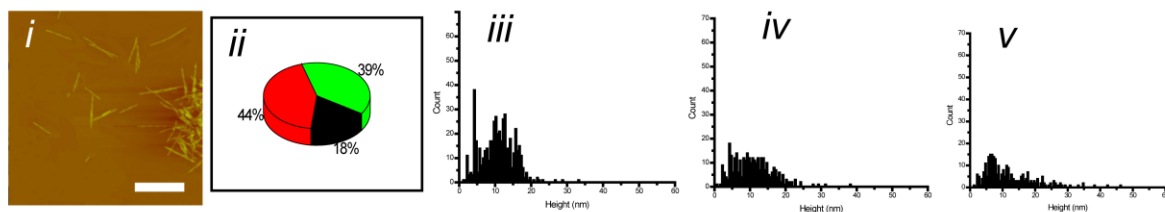
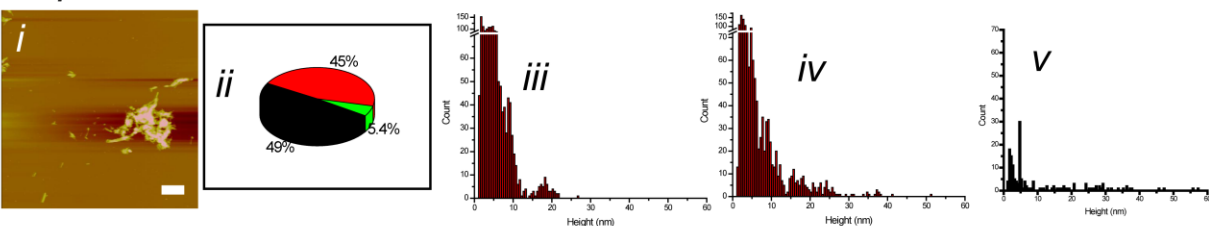


Figure s5. AFM images (indicated with “i”) of the aggregates formed in low salt buffers at pH 2.0 (A), pH3.7 (B), pH 5.6 (C), and pH 7.0 (D). The graphs under “ii” show yields of oligomers (black), protofibrils (red) and long fibrils (green) for the same set of pHs. The panels (iii) – (v) show the heights distributions for the samples obtained at pH 2.0 (A), pH3.7 (B), pH 5.6 (C), and pH 7.0 (D) for oligomers (iii), protofibrils (iv), and fibrils (v).

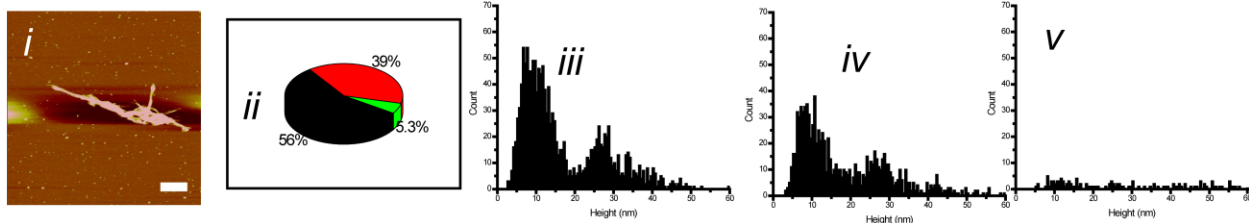
A. pH 2.0



B. pH 3.7



C. pH 5.6



D. pH 7.0

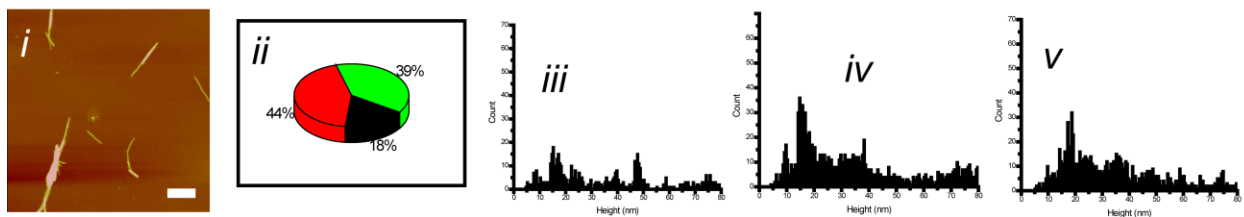


Figure s6. AFM images (indicated with “i”) of the aggregates formed in high salt buffers at pH 2.0 (A), pH3.7 (B), pH 5.6 (C), and pH 7.0 (D). The graphs under “ii” show yields of oligomers (black), protofibrils (red), and long fibrils (green) for the same set of pHs. The panels (iii) – (v) show the heights distributions for the samples obtained at pH 2.0 (A), pH3.7 (B), pH 5.6 (C), and pH 7.0 (D) for oligomers (iii), protofibrils (iv), and fibrils (v).

Table s1. Parameters of dynamic force spectra for proline mutant (Q5P)

Peptide	$k_{\text{off}(1)}(\text{S}^{-1})$	T_1 (S)	ΔG ($K_B T$)	$x_{(1)}(\text{nm})$	$k_{\text{off}(2)}(\text{S}^{-1})$	T_2 (S)	ΔG ($K_B T$)	$x_{(2)}(\text{nm})$
PepQ	11.2 ± 11.5	0.09	27.0	0.16 ± 0.05	46.9 ± 7.6	0.02	25.6	0.003 ± 0.001
PepP	5.6 ± 4.9	0.16	27.7	0.27 ± 0.08	-			-

k_{off} – dissociation rate constant for the peptide-peptide pair, x – the position of energy barrier.

The indices 1 and 2 in the subscript of the parameters refer to the outer and inner barriers of the energy landscape, respectively.